






Modeling Doxorubicin-Induced Cardiomyopathy With Fibrotic Myocardial Damage in Wistar Rats

Ekaterina Podyacheva^{a, b} , Tatiana Shmakova^a, Ekaterina Kushnareva^a, Anatoliya Onopchenko^a, Mikhail Martynov^a, Daria Andreeva^a , Roman Toropov^a , Yuri Cheburkin^a , Ksenia Levchuk^a, Alexandra Goldaeva^a, Yana Toropova^a 

Abstract

Background: Cardiovascular complications, arising after anthracycline chemotherapy, cause a significant deterioration in the life quality and expectancy of those patients who were previously successfully treated for malignant neoplasms. A number of clinical studies have demonstrated that patients with cardiotoxicity manifested during anthracyclines therapy also have extensive fibrotic changes in the cardiac muscle in the long term. Given the lack of an unambiguous understanding of the mechanisms of fibrotic changes formation under doxorubicin treatment in the myocardium, there is the obvious necessity to create a relevant experimental model of chronic doxorubicin-induced cardiomyopathy with fibrotic myocardial lesions and delayed development of diastolic dysfunction.

Methods: The study was divided into two stages: first stage (creation of acute doxorubicin cardiomyopathy) - 35 male Wistar rats; second stage (creation of chronic doxorubicin cardiomyopathy) - 40 male Wistar rats. The animals were split into eight groups (two control ones and six experimental ones), which determined the doxorubicin dose (first stage: 25, 20.4, 15 mg/kg; second stage: 5, 10, 15 mg/kg, intraperitoneally) and the frequency of injection. Echocardiographic, hematological, histological, and molecular methods were used to confirm the successful modeling of acute and chronic doxorubicin-induced cardiomyopathy with fibrotic lesions.

Results: A model of administration six times every other day with a cumulative dose of doxorubicin 20 mg/kg is suitable for evaluation of acute cardiotoxicity. The 15 mg/kg doxorubicin dose is highly cardiotoxic; what's more, it correlates with progressive deterioration of the clinical condition of the animals after 2 months. The optimal cumulative dose of doxorubicin leads to clinical manifestations confirmed by echocardiographic, histological, molecular changes associated with the development of chronic doxorubicin-induced cardiomyopathy

with fibrotic lesions of the left ventricular of the cardiac muscle and ensure long-term survival of animals is 10 mg/kg doxorubicin. A dose of 5 mg/kg of the doxorubicin does not ensure the development of fibrous changes formation.

Conclusion: We assume that cumulative dose of 10 mg/kg with a frequency of administration of six times in 2 days can be used to study the mechanisms of anthracycline cardiomyopathy development.

Keywords: Anthracyclines; Cardiotoxicity; Diastolic dysfunction; Heart failing; Modeling; Myocardial fibrosis

Introduction

Anthracyclines belong to the group of substances, which have both antimicrobial and antitumor activity. These drugs are commonly used for malignant tumors of various origins, such as oncohematological, soft tissue sarcomas, carcinomas, and other solid tumors [1-3]. Daunorubicin was the first anthracycline to be discovered in 1960s; it is naturally produced by an actinobacteria species called *Streptomyces peucetius* [4, 5]. Nowadays, the most clinically important anthracyclines are doxorubicin, daunorubicin, epirubicin, and idarubicin [5].

Side effects after anthracyclines chemotherapy include cardiovascular disease. Development of heart failure causes a considerable deterioration in the quality of life and expectancy of those patients who were previously successfully treated for malignant neoplasms. Doxorubicin is known to induce myocardial cell death through exploiting a variety of mechanisms: apoptosis, autophagy, necroptosis, ferroptosis, and pyroptosis [6-10].

To date, a complete understanding of the mechanisms of anthracycline (doxorubicin) cardiotoxicity development has not been gained. Doxorubicin is able to block the nuclear enzyme topoisomerase II, which controls the topological state of DNA in the cell. Anthracyclines are easily captured by cells and localized in the nucleus [11]. The intercalation function suppresses the synthesis of DNA and RNA in highly replicating cells (anti-cancer effect) and resting cells (cardiomyocytes), subsequently blocking the processes of transcription and replication. Anthracyclines, as DNA intercalators, form a stable ternary anthracycline-DNA-topoisomerase II β com-

Manuscript submitted August 4, 2022, accepted October 26, 2022
Published online December 1, 2022

^aAlmazov National Medical Research Centre, Ministry of Health of the Russian Federation, 197341, Saint-Petersburg, Russian Federation

^bCorresponding Author: Ekaterina Podyacheva, Almazov National Medical Research Centre, Ministry of Health of the Russian Federation, 197341, Saint-Petersburg, Russian Federation. Email: ekaterinapodyachevaspb@gmail.com

doi: <https://doi.org/10.14740/cr1416>

plex, thus “poisoning” the enzyme and preventing re-ligation of double-stranded DNA breaks. Topoisomerase II-mediated DNA damage subsequently stops proliferation and activates the DNA repair mechanism. When the repair process fails, the lesions initiate a programmed cell death [12-14]. Moreover, doxorubicin is able to form reactive oxygen species (ROS). The quinone fragment of anthracyclines can undergo redox reactions with formation of an excess of ROS in the presence of oxidoreductive enzymes, such as cytochrome P450 reductase, NADH dehydrogenase, and xanthine oxidase [15-17]. Conversion of quinone to semiquinone produces free radicals which actively react with oxygen to generate superoxides, hydroxyl radicals and peroxides [2, 3, 18, 19]. Additionally, the availability of cellular iron catalyzes redox reactions and generates ROS. Excessive ROS that cannot be utilized contribute to oxidative stress, DNA damage and lipid peroxidation, thereby causing apoptosis and necrosis [20-23]. All mechanisms ultimately lead to the cardiomyocyte death and proliferation of connective tissue, and cicatricial (fibrotic) changes in the cardiac muscle. However, a number of clinical trials have demonstrated that patients with cardiotoxicity revealed during anthracyclines therapy also have extensive fibrotic changes in the heart muscle in the long term, which worsen the prognoses of such patients [24].

At the moment, the clinic has established the following figures for the incidence of congestive heart failure against the background of the use of appropriate doses of doxorubicin: 4.7% (400 mg/m²), 26% (550 mg/m²) and 48% (700 mg/m²) [14, 25]. Therefore, the cumulative lifetime exposure to doxorubicin is limited to 400 - 450 mg/m² in order to reduce the incidence of heart failure to less than 5%. At the same time, different people have differences in tolerance to doxorubicin. Risk factors that influence the degree of anthracycline-induced cardiac injury include genetic variation [26], age (younger or older age groups), previous treatment with cardiotoxic drugs, and a history of heart disease [27]. Children are particularly at risk due to anthracycline activity, which can compromise the development of an immature heart. The exact mechanism for the development of cardiotoxicity remains unclear, due to the poorly understood mechanisms of anthracyclines action.

Researching genetic mechanisms of fibrosis formation in the doxorubicin-induced cardiomyopathy development remains relevant. The following is being researched: transforming growth factor (TGF)- β signaling pathway and its effect on *COL* type I, II and III gene expression, interaction of TGF- β with fibroblast growth factors (FGF) [28, 29], contribution of inflammatory tumor necrosis factor (TNF)- α [30, 31], participation of alpha-smooth muscle actin (α -SMA) [32], the role of matrix metalloproteinases (MMP) and their inhibitors, tissue inhibitor of metalloprotease (TIMP) [33], and factors, which additionally regulate fibroblast activity, such as endothelin (ET)-1, adrenaline, and angiotensin 2 [34].

Despite the numerous researches about chronic doxorubicin-induced cardiomyopathy modeling, the attention was mainly focused on the clinical criteria of cardiac dysfunction (decreased ejection fraction, increased markers of myocardial damage) and such histological patterns as structural damage in the myocardium and tissue edema [15]. The effects of free

radicals due to the activation of oxidative stress during anthracyclines therapy not only damage the heart tissue, but also involve the kidneys in a pathological process with subsequent impairment of their function [35]. Doxorubicin has a harmful effect on the glomeruli, leading to severe proteinuria [36, 37]. Affected by a persistent systemic inflammation and activation of oxidative stress proteinuria [38], in its turn, leads to fibrotic changes in the kidneys, which can further significantly impair their function [39]. Thus, it is observed a close relationship between pathophysiological changes in the renal function and such changes in the cardiac function during the development of heart failure, and the peculiarities of modern cardioprotective therapy against the background of doxorubicin treatment, which includes therapy with drugs belonging to the group of renin-angiotensin-aldosterone system (RAAS) blockers. The modern chronic doxorubicin-induced cardiomyopathy experimental model should consider not only characteristic changes in the myocardial function, including an assessment of the degree of fibrosis, but also the background state of the renal excretory system.

To date, a lot of data have been published to be devoted to the doxorubicin-induced cardiomyopathy modeling using various animal species [15, 40-46]. Nevertheless, taking into account the lack of an unambiguous understanding of the mechanisms of the fibrotic changes formation in the cardiac muscle under the influence of doxorubicin, consequently, a relevant experimental model of chronic doxorubicin-induced cardiomyopathy with fibrotic lesions of the heart muscle is in great demand. Creating a relevant model that meets modern conditions will allow developing new pathogenetical approaches to treatment and prevention, to improve the life quality and expectancy of patients undergoing chemotherapy.

The study was aimed to create an acute and chronic doxorubicin-induced cardiomyopathy with fibrous lesion of the left ventricle and delayed development of diastolic dysfunction in Wistar rats. Furthermore, the task to determine the main molecular markers involved in fibrous tissue formation in the chronic doxorubicin-induced cardiomyopathy development.

Materials and Methods

Pharmacological agents

Doxorubicin-LENS[®], 50 mg (VEROPHARM, LLC, Russia) was used to create the model. The drug was prepared for administration to animals immediately before use (*ex tempore*). Doses of the drug were determined empirically, taking into account literature data. The dose of the drug calculated for each animal was diluted with saline. During the experiment, the animals were periodically weighed and the doses of the drug were adjusted.

Ethical approval

The study in animal protocol was approved by a bioethical

Table 1. Brief Description of the Experimental Groups

Group, n	The route of administration	Dose	Frequency of administration	Cumulative dose
The first stage - modeling of acute doxorubicin cardiomyopathy				
DOX-25 (n = 10)	IP	2.5 mg/kg	Ten times over 1.5 weeks given every day	25 mg/kg
DOX-20.4 (n = 10)	IP	3.4 mg/kg	Six times over 1.5 weeks given every other day	20.4 mg/kg
DOX-15 (n = 10)	IP	2.5 mg/kg	Six times over 1.5 weeks given every other day	15 mg/kg
Control (n = 5)	IP	1 mL 0.9% sodium chloride	Six times over 1.5 weeks given every other day	6 mL
The second stage - modeling of chronic doxorubicin cardiomyopathy				
DOX-15 (n = 10)	IP	2.5 mg/kg	Six times over 2.5 weeks given in 2 days	15 mg/kg
DOX-10 (n = 10)	IP	1.67 mg/kg	Six times over 2.5 weeks given in 2 days	10 mg/kg
DOX-5 (n = 10)	IP	0.83 mg/kg	Six times over 2.5 weeks given in 2 days	5 mg/kg
Control (n = 10)	IP	1 mL 0.9% sodium chloride	Six times over 2.5 weeks given in 2 days	6 mL

IP: intraperitoneally.

commission of the Centre for Experimental Biomedicine, Institute of Experimental Medicine, Almazov National Medical Research Centre, Ministry of Health of the Russian Federation (No. 20-09П3#V2, date of approval: 25.06.2020). The study was conducted according to the guidelines of the Declaration of Helsinki.

Experimental model

The development of models was carried out in two successive stages: first stage (creation of acute doxorubicin-induced cardiomyopathy) - 35 male Wistar SPF rats weighing 393 ± 38 g (5 months); second stage (creation of chronic doxorubicin-induced cardiomyopathy) - 40 male Wistar SPF rats weighing 260 ± 19 g (3 months). In the first stage, rats with a greater weight were involved, due to the stronger effect of the chemotherapy drug. Animals were housed in a barrier-type vivarium under standardized conditions for animal facilities: 12-h light/dark cycle with food and water *ad libitum*. Animals were randomly divided into groups with a certain frequency of intraperitoneally administration and a certain dose of doxorubicin (Table 1).

Stage I: modeling of acute doxorubicin-induced cardiomyopathy

At the first stage of the study, echocardiography (ECHO) was recorded before the start of the chemotherapeutic agent injection and 2 days after the end of the injection. The next day, under isoflurane anesthesia (5% isoflurane-98% oxygen), vital organs, heart and kidneys, were taken. Before cardiac arrest, 10% KCl solution was injected into the left ventricle until cardiac arrest was completed in the diastole phase.

Stage II: modeling of chronic doxorubicin-induced cardiomyopathy

The second stage of the study included four discrete points: starting point (indicates the phase before the doxorubicin injection), 0 point (demonstrates the completion of the doxorubicin injection), first month and second month (Fig. 1). At each point, ECHO was performed and blood was taken from the retroorbital sinus for hematological analysis. Intravital blood samples, which were taken from the retroorbital sinus (0.25

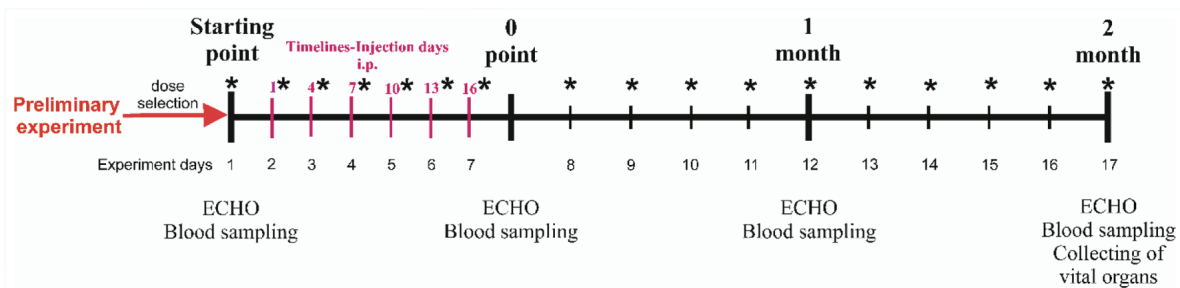


Figure 1. Experiment scheme. *Weighing points. IP: intraperitoneally.

mL), were performed under isoflurane anesthesia. In the subsequent stage, autopsy was performed on the animal under xylazine anesthesia (10 mg/kg xylazine + 25 mg/kg zoletil, intramuscularly), and the heart and the kidneys were removed for histological analysis. During the procedure, 10% KCl solution was injected into the left ventricle as long as the cardiac arrest happened. After removal of the heart from the chest cavity, the heart apex was cut off and subjected to deep freezing (-80 °C) for further performing of RT-qPCR.

From the starting point until 0 point, the animals were weighed every 2 days, then once a week (Fig. 1). In order to assess the change in the body weight, an AND DX 1200 WP electronic laboratory scale (Japan) with an accuracy of 0.01 g was used.

Echocardiography

Before echocardiography, the animal was anesthetized using an inhalation mixture of 1.7% isoflurane-98% oxygen. The echocardiographic images were obtained with heart rate stabilized at about 400 beats per minute. Echocardiogram was recorded using The Vevo[®] 2100 (VisualSonics Inc., Toronto, Canada). All parameters were taken from the right parasternal short axis. The analysis of the myocardium functioning parameters was carried out in the M mode. Left ventricular end-diastolic internal diameter at Q wave (LVIDd), left ventricular end-systolic internal diameter at T wave (LVIS), posterior wall thickness at diastole (LVPW), and anterior wall thickness at diastole (IVS) were measured. Another parameter was calculated as follows: left ventricular short axis fractional shortening FS (%) = (LVIDd - LVIS)/LVIDd × 100.

Morphometric studies

The heart and the kidneys were excised and fixed in 10% formaldehyde solution for 72 h. The tissue samples were encased in paraffin. In order to study the morphological changes, 3-μm thick cross-sections were made using rotary microtome Accu-Cut SRM (Sakura, Japan). The sections were stained by hematoxylin and eosin, dehydrated and enclosed in a synthetic mounting medium (Biovitrum, St. Petersburg, Russia). Morphometric studies were carried out on micrographs of the samples stained by Mallori using a Nikon Eclips 400i microscope (Nikon, Tokyo, Japan) and NIS Elements 4.3 Br software (Nikon, Tokyo, Japan). For each animal, there were five randomly selected fields of view on each histological section. Five photographs of the left ventricular (LV) of the cardiac muscle were taken at × 400 magnification. In each micrograph, the amount of collagen-stained blue was counted and expressed as a percentage of the total section area using Photoshop CS6 (Adobe Inc., California, USA). Graphically, the data were expressed as a range chart.

Hematology

A general blood test was performed using an Abacus junior

Vet (Diatron, Budapest, Hungary) veterinary hematological analyzer. Quantitative parameters were evaluated. The following blood ones were determined: white blood cells (WBCs, g/L); leukocyte fraction: granulocytes (Gr, %), lymphocytes (Lym, 10⁹ g/L), monocytes (Mi, %), red blood cells (RBCs, × 10¹²/L), hemoglobin (Hb, g/L); erythrocyte indices: mean concentration hemoglobin (MCH, pg), mean corpuscular hemoglobin concentration (MCHC, g/L), mean corpuscular volume (MCV, fL), hematocrit (Hct, %), and platelets (Plt, × 10⁹/L).

RNA extraction and RT-qPCR

The total RNA was extracted from deep frozen heart apex samples using ExtractRNA[™] solution and CleanRNA Standard[™] Kit (Evrogen JSC, Russia) according to the manufacturer's protocols. Reverse transcription (RT) and consequent quantitative real-time PCR (qPCR) were performed using OneTube RT-PCR SYBR[™] Kit (Evrogen, JSC, Russia) following the manufacturer's instructions. RT-qPCR was performed by a Bio-Rad CFX96 thermocycler (Bio-Rad, Hercules, CA). The parameters for RT-qPCR were set as follows: initial heating at 95 °C for 1 min and then followed by 40 cycles with denaturation at 95 °C for 15 s, annealing at 60 °C for 20 s, and extension at 72 °C for 60 s. Relative expressions of 13 genes of interest and four housekeeping genes were calculated by the 2^{-ΔΔC_t} method and normalized by GAPDH, α-tubulin, β-actin and TBP. The primer sequences are listed in Table 2.

Statistical analysis

All calculations were performed with GraphPad Prism 8 (GraphPad Software, Inc., San Diego, CA, USA) software for Windows (Microsoft Inc., USA). The Shapiro-Wilk test was used to detect the normal distribution. An unpaired, non-parametric Kruskal-Wallis test with Dunn's test was used to compare between several independent groups, since the data obtained (ECHO and hematological values) are non-normally distributed. The Wilcoxon test was used for pairwise comparison of dependent values of the non-normal distribution (ECHO data, *dynamics compared to the initial value). An unpaired, non-parametric Kruskal-Wallis test with Dunn's test was used to compare the body weight of animals and assess the histological differences between different groups. The values in the groups were processed using nonparametric statistics (median and 25th and 75th percentiles (Me (25-75%))). One-way analysis of variance (ANOVA) followed by Tukey's *post-hoc* test was used for statistical analysis of RT-qPCR data. The values are shown as mean ± standard deviation (SD). The differences were considered significant at P < 0.05.

Results

Modeling of acute doxorubicin-induced cardiomyopathy

There was a 100% death of animals observed against the back-

Table 2. Lists of Primer Sequences Used for RT-qPCR

Genes	Primers	Sequences (5'-3')
ACTA (α -SMA)	Forward	CACCGCTGAACGTGAAATTG
	Reverse	CTTCTCCAGAGAGGAGGAAG
TGF- β 1	Forward	GACTCTCCACCTGCAAGACC
	Reverse	GGACTGGCGAGCCTTAGTTT
FGF2	Forward	TCCATCAAGGGAGTGTGTGC
	Reverse	TCCGTGACCGGTAAGTGTG
FGF4	Forward	CTACCTGCTGGGCCTCAAAA
	Reverse	CACACCCCGCTGCTGTC
Col1a1	Forward	GTGGATGGCTGCACGAGTC
	Reverse	GAGTTTGGGTTGTTGGTCTG
Col2a1	Forward	GCTGTGGAAGTGGATGAAGA
	Reverse	GAGGAACTGTGGAGAGACG
Col3a1	Forward	CAGGCCAATGGCAATGTAAAG
	Reverse	CATCCTCTAGAACTGTGTAAG
TNF- α	Forward	GGCTCCCTCTCATCAGTTC
	Reverse	CTGCTTGGTGGTTTGTCTAC
ET-1 (endothelin-1)	Forward	TGATTCTTTGCCTCTTCTTG
	Reverse	TATGGAATCTCCTGGCTCTC
TIMP-1	Forward	CTGAGAAGGGCTACCAGAG
	Reverse	GTCATCGAGACCCCAAGGT
TIMP-2	Forward	GGACCTGACAAGGACATCG
	Reverse	TTCTTTCCTCCAACGTCCAG
MMP-1	Forward	GATGAAAGGTGGACCAACAAT
	Reverse	CCAAGAGAATGGCCGAGTTC
MMP-2	Forward	TGGGGGAGATTCTCACTTG
	Reverse	CCATCAGCGTCCCATACTT
MMP-14	Forward	TGGGGTCATCTGCTTCTCTT
	Reverse	TAGGGCTCATATGCCCAAAG
Housekeeping genes	Primers	Sequences (5'- 3')
GAPDH	Forward	CAAGTTC AACGGCACAGTCA
	Reverse	CATACTCAGCACCAGCATCA
α -tubulin	Forward	CAATTCCATCCTCACCACC
	Reverse	CAACCTGTTTAAGTTAGTGTAG
TBP (TATA-box binding protein)	Forward	TGCGTTGATCTTCAGTTCTG
	Reverse	CTTGCTGCTAGTCTGGATTG
ACTB (β -actin)	Forward	GGTGTGATGGTGGGTATGG
	Reverse	GTTGGTGACAATGCCGTGTT

α -SMA: alpha-smooth muscle actin; MMP: matrix metalloproteinases; TIMP: tissue inhibitor of metalloprotease; TGF: transforming growth factor; FGF: fibroblast growth factors; TNF: tumor necrosis factor; RT-qPCR: reverse transcription quantitative real time polymerase chain reaction.

ground of the injection of the drug at a dose of 25 mg/kg, while when using a lower dose (20.4 mg/kg), the death of animals was 30%. Mortality in the control and DOX-15 groups animals was not observed. The decrease in body weight on the

background of doxorubicin administration was: 68 ± 14.6 g of the DOX-25 group of animals; 58.8 ± 12.2 g of the DOX-20.4 group of animals; 56.3 ± 17.4 g of the DOX-15 group of animals.

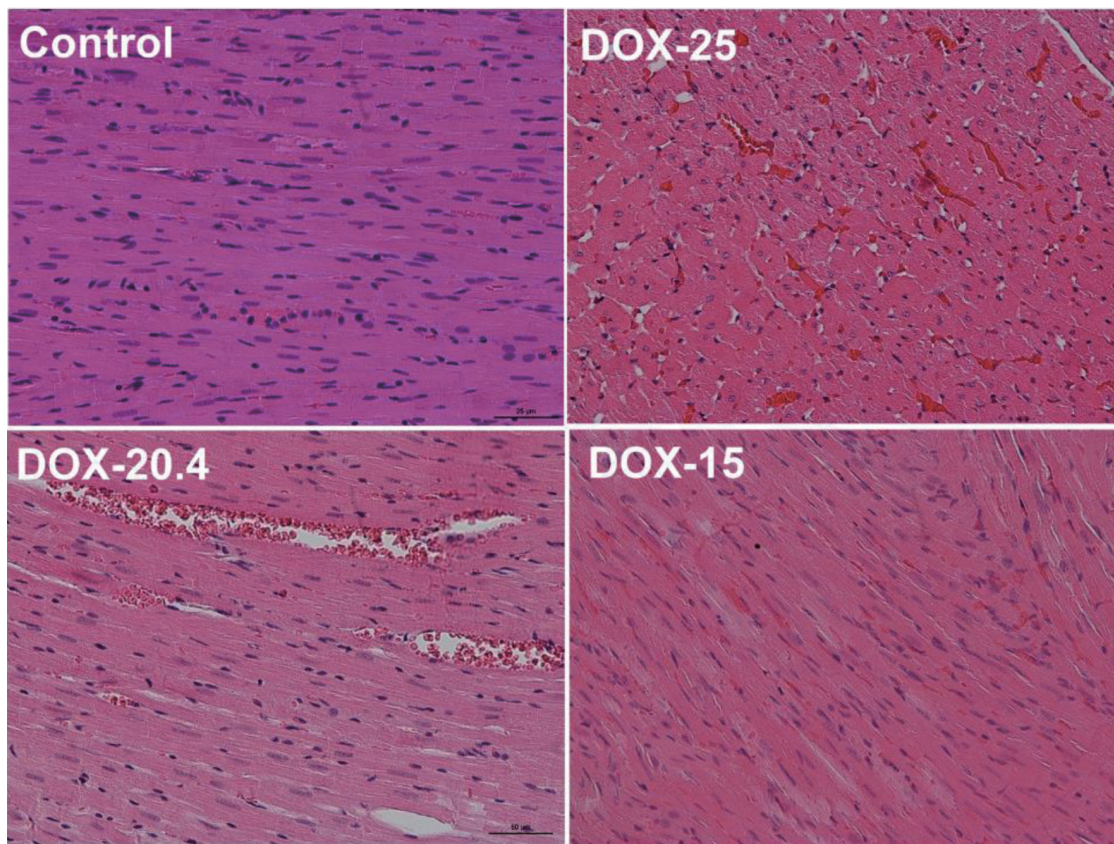


Figure 2. Representative images of rat's left cardiac ventricle of the control, DOX-25, DOX-20.4, and DOX-15 groups. Stained by hematoxylin and eosin, $\times 50$.

Due to the extremely severe physical condition such as substantial weight loss over 20% in a short period of time, abundant discharge of porphyrin, decreased physical activity, alteration of the consistency of feces to jelly-like and high mortality, ECHO was not possible in animals receiving 25 and 20.4 mg/kg cumulative doses of the drug. There were a significant decrease in the FS (before: $54.5 \pm 5.9\%$; after: $37.5 \pm 5.5\%$; $***P \leq 0.001$) and an increase in the LVIDs (before: 3.1 ± 0.53 mm; after: 4.1 ± 0.37 mm; $***P \leq 0.001$) on the 13th day after the start of doxorubicin injection at a dose of 15 mg/kg.

The histopathological picture of the heart muscle of the left ventricle revealed capillary plethora and dilated vessels in all animals treated with doxorubicin, the most pronounced in animals receiving the maximum cumulative dose (25 mg/kg). They are also characterized by a partial loss of myofibrils of cardiomyocytes (Fig. 2). The picture of damage to the tissues of the kidneys was characterized by hemorrhage in the medulla of the kidney, compressed and deformed nephrons. Venous plethora of the cortical and medulla of the kidneys, moderate atrophy of the tubules (decrease in the height of epithelial cells and widening of the lumen of the tubules) and necrosis of individual epitheliocytes were revealed in animals receiving 25 mg/kg of the drug (Fig. 3).

Thus, the use of 20 and 25 mg/kg of doxorubicin ensures the development of acute cardiotoxic effects, manifested in a pronounced deterioration in the physical and clinical condition

of the animals. A dose of 15 mg/kg of the drug was used to model chronic doxorubicin-induced cardiomyopathy.

Modeling of chronic doxorubicin-induced cardiomyopathy

There was a 30% death rate noted in animals 45 days after the last injection of the drug when using the maximum cumulative dose (15 mg/kg). There were no deaths in the other groups.

The dynamics of body weight of animals in all experimental groups is shown in Figure 4. A gradual increase in body weight was observed during the entire experiment in the control group of animals and in the DOX-5 group. Weight loss was observed during injections in the surviving animals using the maximum cumulative dose (DOX-15). In the DOX-15 group of animals, a rapid deterioration in the clinical state characterized by substantial weight loss, abundant discharge of porphyrin, and decreased physical activity of the animals was observed, which led to their earlier withdrawal from the experiment.

No changes in the echocardiography parameters were observed during the experiment in the control group animals.

There was a significant increase in the LVIDs and LVIDd in animals after the injection of all doses ($P < 0.05$, compared to the initial value, compared to the control group). Besides, a significant decrease in the FS was observed in all experimental

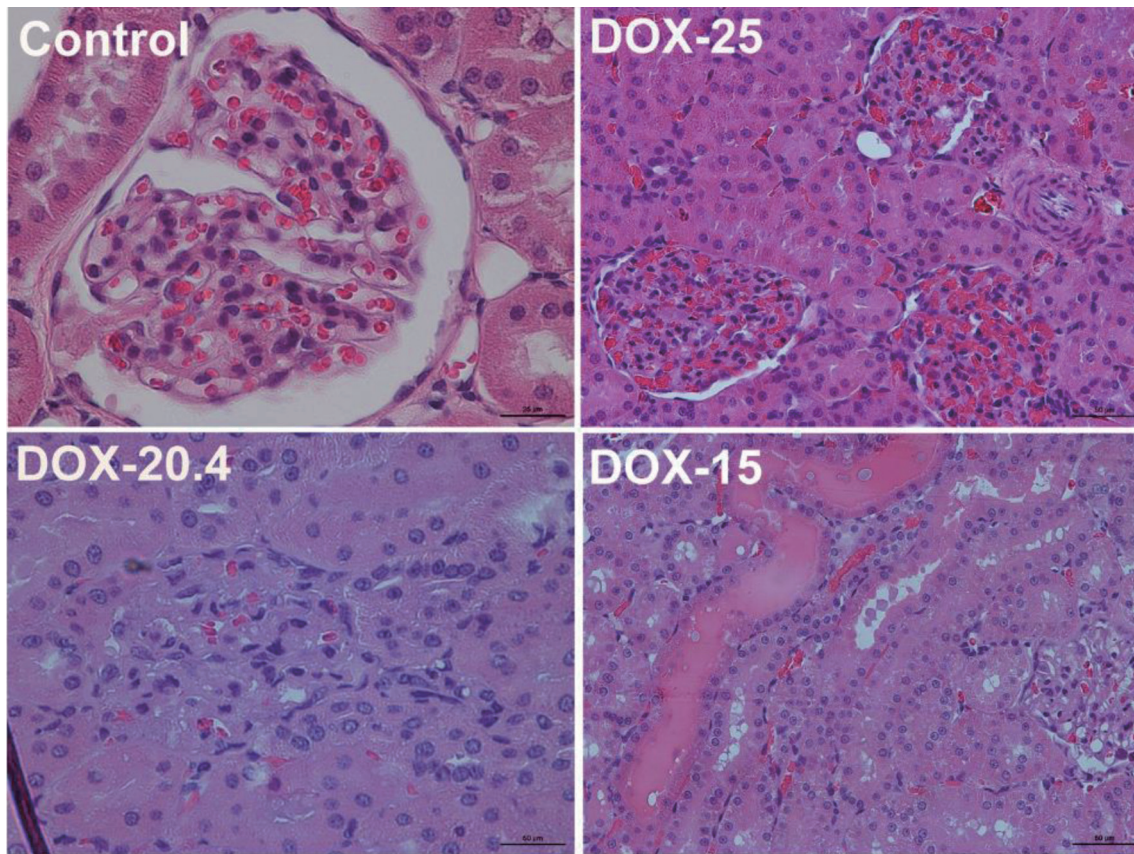


Figure 3. Representative images of rat's kidney of the control, DOX-25, DOX-20.4, and DOX-15 groups (stained by hematoxylin and eosin, $\times 25$ (control group); $\times 50$ (DOX-25, DOX-20.4, and DOX-15 groups)).

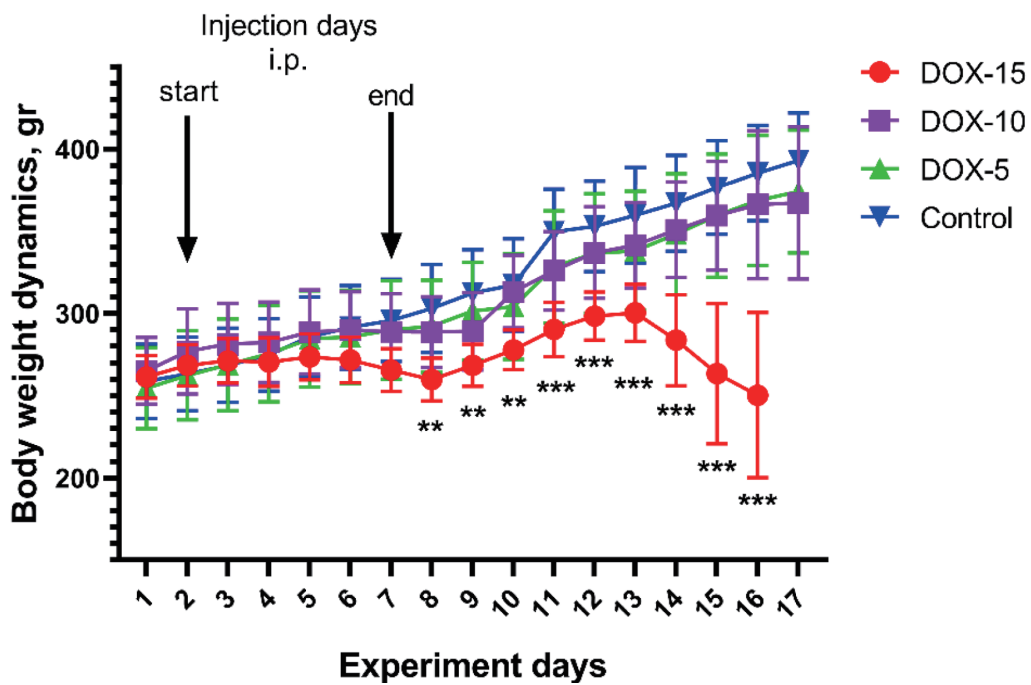


Figure 4. Dynamics of body weight in animals of the DOX-15, DOX-10, and DOX-5 groups. *Significant differences between the DOX-15 group of animals versus the DOX-10, DOX-5, and control groups (** $P < 0.01$, *** $P < 0.001$).

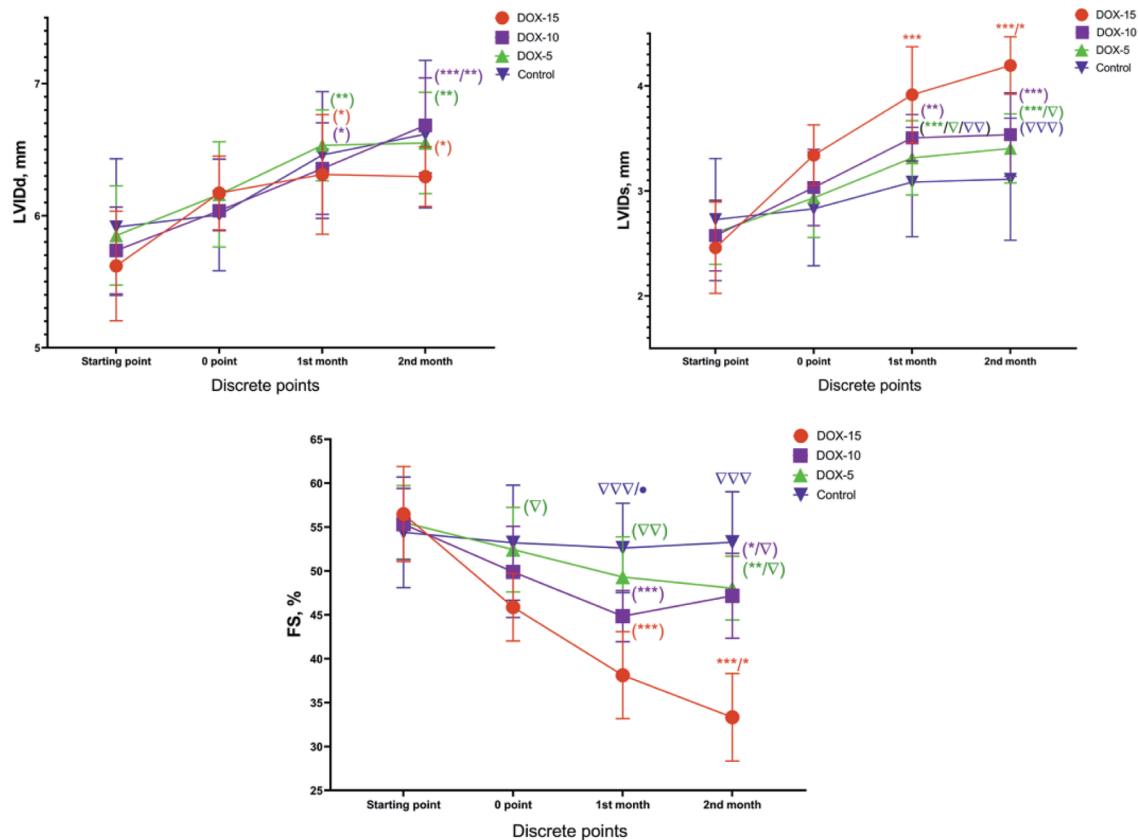


Figure 5. LVIDs, LVIDd and FS dynamics of animals of the DOX-15, DOX-10, and DOX-5 groups. *Dynamics compared to the initial value (e.g., in the DOX-15 group; *P < 0.05, **P < 0.01, ***P < 0.001). Δ: dynamics compared to the highest dose at each point of the experiment (e.g., in first month: DOX-5, control vs. DOX-15; Δ: P < 0.05, ΔΔ: P < 0.01, ΔΔΔ: P < 0.001). LVIDs: left ventricular end-systolic internal diameter; LVIDd: left ventricular end-diastolic internal diameter; FS: fractional shortening.

groups (Fig. 5). The most substantial decrease in FS (41% of the initial value) was observed in animals after the injection of the maximum cumulative dose of the drug (DOX-15). Whereas for the group of animals receiving 10 mg/kg, a decrease in FS by 15% was noted, and 14% in the DOX-5 group of animals.

A slight increase in the dimensions of the anterior (IVS) and posterior (LVPW) walls thickness in left ventricular diastole was revealed in the animals receiving 10 and 5 mg/kg cumulative doses (Fig. 6). A significant increase in both IVS and LVPW was found between the animals of the DOX-10 and DOX-5 groups compared to the DOX-15 group (P < 0.05). Depletion of both the anterior and posterior walls thickness of the left ventricle was observed during the drug injection in animals receiving a cumulative dose of 15 mg/kg of doxorubicin by the end of the second month.

The results of a general blood test showed a significant decrease after the drug injection (0 point) in such indicators as WBC, Lym, GR, Mi, Hb, MCH, and MCHC in animals of the DOX-15 and DOX-10 groups compared to the control group (Table 3). It can be assumed that these changes are associated with the acute toxic effect of anthracycline in the form of inhibition of hematopoiesis in animals that received the highest doses. After a month, the values of hematological parameters returned to normal ones, which indicates the reversibility of

this effect.

Histology of the left cardiac ventricle tissue in animals with chronic doxorubicin-induced cardiomyopathy revealed foci of cardiomyocytes with pronounced vacuolization of the cytoplasm and hemorrhages at the sites of necrosis. The heart muscle of animals receiving 10 and 5 mg/kg was less damaged, but at the same time, there was also a partial loss of nuclei, vacuolated cytoplasm and necrosis of contraction bands, which is a sign of focal necrosis at the stage of cell decay with destruction of the vascular wall and minor hemorrhage (Fig. 7). Stained by Mallori of the left cardiac ventricle revealed an increase in the percentage occupied by collagen in animals receiving 15 and 10 mg/kg of doxorubicin compared to the control group (DOX-15: 11.42% (9.920; 13.61); DOX-10: 7.77% (4.35; 10.84); DOX-5: 5.42% (4.568; 6.408); control: 3.23% (2.465; 3.620)) (Figs. 8, 9). The histopathological picture of the kidney tissue showed the presence of segmental glomerulosclerosis and tubular epithelial necrosis most pronounced in animals treated with 15 mg/kg doxorubicin (Fig. 10).

The disorders ultimately lead to the pronounced fibrosis development of the left ventricular of the cardiac muscle within 2 months in the animals that received 10 mg/kg of anthracycline. There is no statistically significant increase in the percentage of fibrous tissue of the cardiac muscle in rats treated

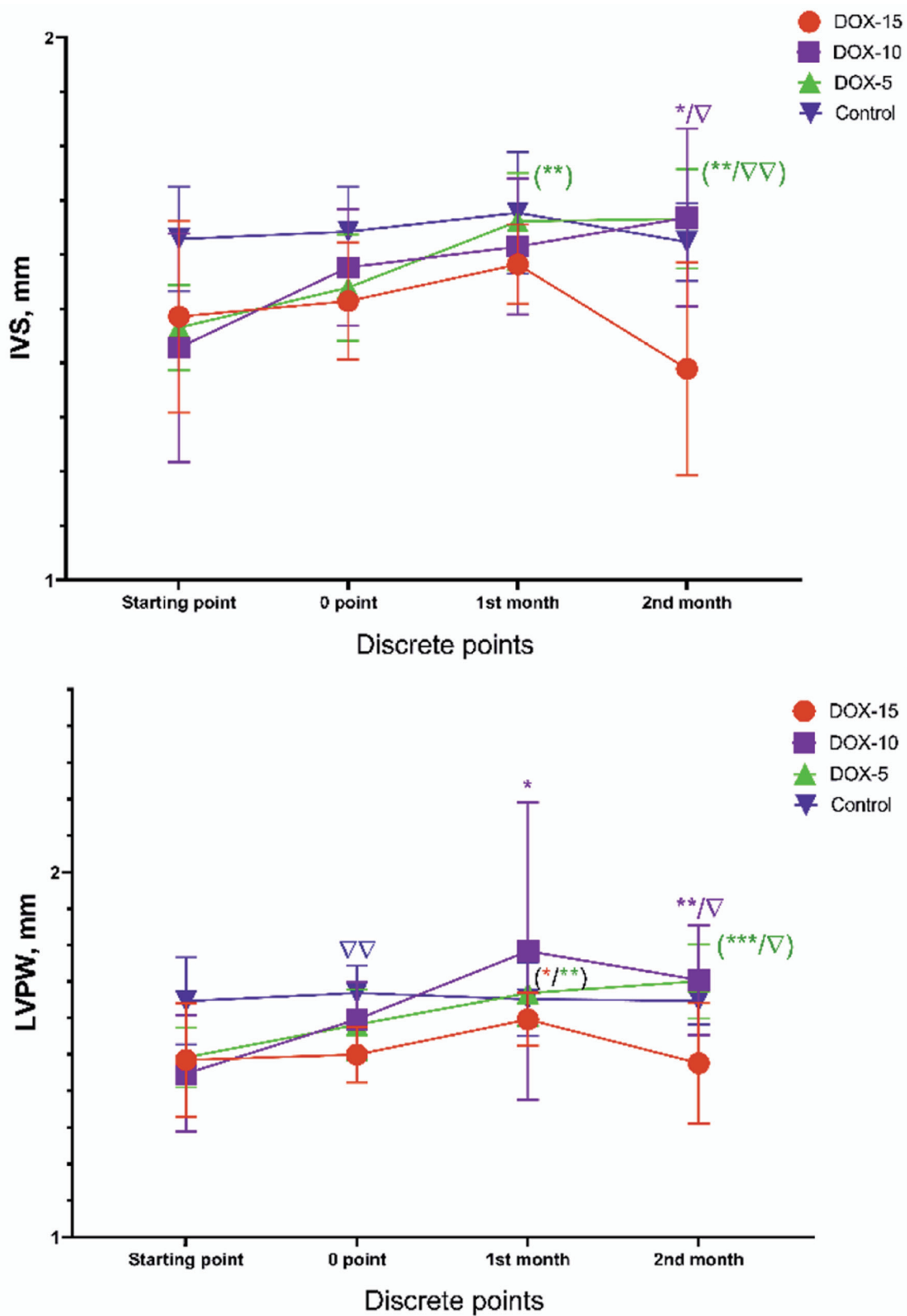


Figure 6. IVS and LVPW dynamics of animals of the DOX-15, DOX-10, and DOX-5 groups. *Dynamics compared to the initial value (*P < 0.05, **P < 0.01, ***P < 0.001). Δ: dynamics compared to the highest dose at each point of the experiment (e.g., in the second month: DOX-10, DOX-5 vs. DOX-15; Δ: P < 0.05, ΔΔ: P < 0.01). IVS: the dimensions of the anterior wall thickness; LVPW: the dimensions of the posterior wall thickness.

Table 3. Quantitative Indicators of Hematological Analysis of Animals of the DOX-15, DOX-10, DOX-5 Groups

Time	Groups			
	DOX-15	DOX-10	DOX-5	Control
WBCs, × 10 ⁹ g/L				
Starting point	9.4 (7.8 - 13.7)	13.3 (7.7 - 17.3)	10.7 (7.6 - 12.7)	9.1 (8.2 - 12.9)
0 point	6.1 (4.7 - 7.4)**	10.3 (7.4 - 11.7)	7.9 (5.7 - 10.1)	12.2 (9.5 - 13.6)
First month	11.4 (7.7 - 15.5)	13.8 (13 - 14.9)	12.7 (10.3 - 12.8)	10.3 (8.5 - 13.3)
Second month	6.3 (4.1 - 7.1)	6.9 (4.9 - 11.3)	7.9 (6.3 - 9.5)*	11.2 (3.8 - 6.3)
Lym, × 10 ⁹ g/L				
Starting point	7.1 (4.8 - 7.9)	6.2 (5 - 8.9)	8.1 (6.2 - 8.2)	7.1 (6.3 - 7.8)
0 point	3.8 (3 - 7.5)**	6.9 (5.3 - 7.9)	5.6 (4.7 - 7.8)	8.9 (7.3 - 9.8)
First month	6.8 (5.9 - 8.4)	10.5 (8.7 - 11.7)	10 (7.2 - 10.9)	7.9 (6.6 - 10.1)
Second month	3.1 (2.8 - 6)	5.7 (3.8 - 7.4)	5.6 (4.2 - 7.1)	7.6 (2.8 - 4.4)
Mi, %				
Starting point	8.9 (7 - 10.3)	4.0 (0.5 - 9.9)	7.5 (0.6 - 13)	1.4 (0.6 - 8.1)
0 point	0.7 (0.6 - 2.6)	0.6 (0.6 - 0.7)**	3.1 (0.6 - 5.4)	4.4 (2.9 - 7)
First month	9 (3 - 11.4)	4.4 (1.2 - 12.3)	4.2 (3 - 12)	3.8 (3.2 - 10.4)
Second month	2.8 (1.9 - 9.5)	7.3 (3.1 - 9.7)	4.9 (2.8 - 9.8)	8.7 (6.4 - 9.8)
GR, %				
Starting point	20.9 (18.3 - 24.5)	14.2 (13.4 - 21.1)	14.2 (8.5 - 18.8)	13.3 (9.2 - 18.8)
0 point	29.8 (24.1 - 35.8)	26.7 (20.6 - 31.3)	17.5 (14.5 - 20.4)	19.6 (16.3 - 23.8)
First month	19 (17.6 - 38.8)	17.9 (15.8 - 21.6)	16.4 (10.4 - 20)	15.4 (14.3 - 19.1)
Second month	12.7 (9.2 - 39.3)	16.8 (14.1 - 19.4)	22.80 (18.1 - 25.5)	24.85 (20.5 - 28.6)
RBCs, 10 ¹² /L				
Starting point	8.3 (7.4 - 8.9)	8 (7.9 - 8.5)	9.6 (8.7 - 9.9)	9.4 (8.7 - 9.7)
0 point	8.6 (8.1 - 9.3)	9.6 (9.2 - 10.6)	8.8 (8.4 - 9.1)	8.7 (8.2 - 9.3)
First month	8.1 (7.7 - 8.5)	8.2 (6.9 - 8.8)	9.7 (9.4 - 10.6)	8.6 (8.3 - 9.6)
Second month	7.7 (6.8 - 8.8)	8 (7.6 - 8.7)	7.9 (7.7 - 8.2)	7.5 (7.2 - 7.7)
Hb, g/L				
Starting point	174 (156 - 189)	166 (160 - 170.5)	168.5 (157.5 - 173.8)	167 (158.5 - 170.3)
0 point	134 (128.3 - 139.8)**	161 (154 - 165)	161 (155 - 164.3)	169 (162 - 172)
First month	169 (164 - 183.5)	177 (169 - 189.5)	169 (164 - 171)	168 (165.5 - 178.3)
Second month	154 (134 - 190.5)	170 (166 - 176.5)*	155.5 (152 - 160.8)	156 (150.8 - 160)
Hct, %				
Starting point	43.4 (38.85 - 45.47)	40.9 (39.66 - 45.82)	46.9 (44.8 - 48.7)	44.2 (41.8 - 46.6)
0 point	42.5 (40.2 - 47.3)	48.8 (46.8 - 49.2)	40.1 (37.5 - 42.7)	42.7 (39.1 - 44.9)
First month	39.5 (38.2 - 42.2)	41.9 (39.5 - 45.4)	47.9 (45.8 - 50.4)	40.4 (38.7 - 44.9)
Second month	34.5 (29.2 - 43.7)	38.1 (36.7 - 39.9)**	35.2 (34.8 - 36.1)	41.1 (33.4 - 35.3)
MCV, fL				
Starting point	52 (51 - 52)	51 (50 - 54)	47.5 (46.7 - 51.)	48 (47 - 49)
0 point	50 (50 - 50.7)	51 (48 - 51.5)	45 (45 - 45.7)	48 (46 - 50)
First month	50 (46.5 - 51.5)	50 (47.7 - 53)	48 (47 - 50)	47 (46.2 - 49.5)
Second month	46 (42.5 - 50)	47.5 (46 - 51)	44.5 (42.7 - 45)	46 (45 - 46)
MCH, pg				

Table 3. Quantitative Indicators of Hematological Analysis of Animals of the DOX-15, DOX-10, DOX-5 Groups - (continued)

Time	Groups			
	DOX-15	DOX-10	DOX-5	Control
Starting point	21 (21 - 21.2)	20.2 (19.3 - 21.3)	17 (16 - 18.6)	17.9 (16.6 - 19.2)
0 point	15.6 (14.4 - 17.4)**	16.9 (14.7 - 18.2)*	18.1 (17.6 - 18.9)	19.2 (18.3 - 19.8)
First month	21.2 (20.3 - 21.9)	21.8 (20.5 - 22.1)*	17 (16 - 17.7)	19.3 (18.4 - 19.9)
Second month	20.6 (19.4 - 21.7)	21.7 (20.3 - 22)	19.6 (19.4 - 19.4)*	20.6 (20.3 - 21.7)
MCHC, g/L				
Starting point	406 (401 - 412)	406 (357 - 422)	363 (340 - 373.8)	384 (343 - 399.5)
0 point	307.5 (292.3 - 350.3)*	327 (306.5 - 349.5)	392 (383 - 403)	395.5 (368 - 403.8)
First month	437 (424.5 - 443.5)	423 (414.8 - 428)	351 (340 - 357)	411.5 (364.3 - 430)
Second month	445 (435.5 - 457.5)	446.5 (437.3 - 459.3)	445.5 (439.3 - 455.8)	453.5 (446.5 - 462.5)
Plt, 10 ⁹ g/L				
Starting point	579 (566 - 649)	628 (572 - 820)	775.5 (689 - 862)	785.5 (785 - 786)
0 point	1,722 (1,358 - 1,816)***	967 (852 - 1,051)	709.5 (654.5 - 746.3)	644 (483 - 659.5)
First month	497.5 (409.8 - 626)	558 (510.3 - 681)	727 (593 - 820)	687 (531 - 731)
Second month	512 (437 - 643)	569 (482 - 592.8)	550 (479.5 - 567.5)	580 (564 - 616.8)

*DOX-15, DOX-10, DOX-5 vs. control (*P < 0.05, **P < 0.01, ***P < 0.001). GR: granulocytes; Hb: hemoglobin; Hct: hematocrit; Lym: lymphocytes; MCH: mean concentration hemoglobin; MCHC: mean corpuscular hemoglobin concentration; MCV: mean corpuscular volume; Mi: monocytes; Plt: platelets; RBCs: red blood cells; WBCs: white blood cells.

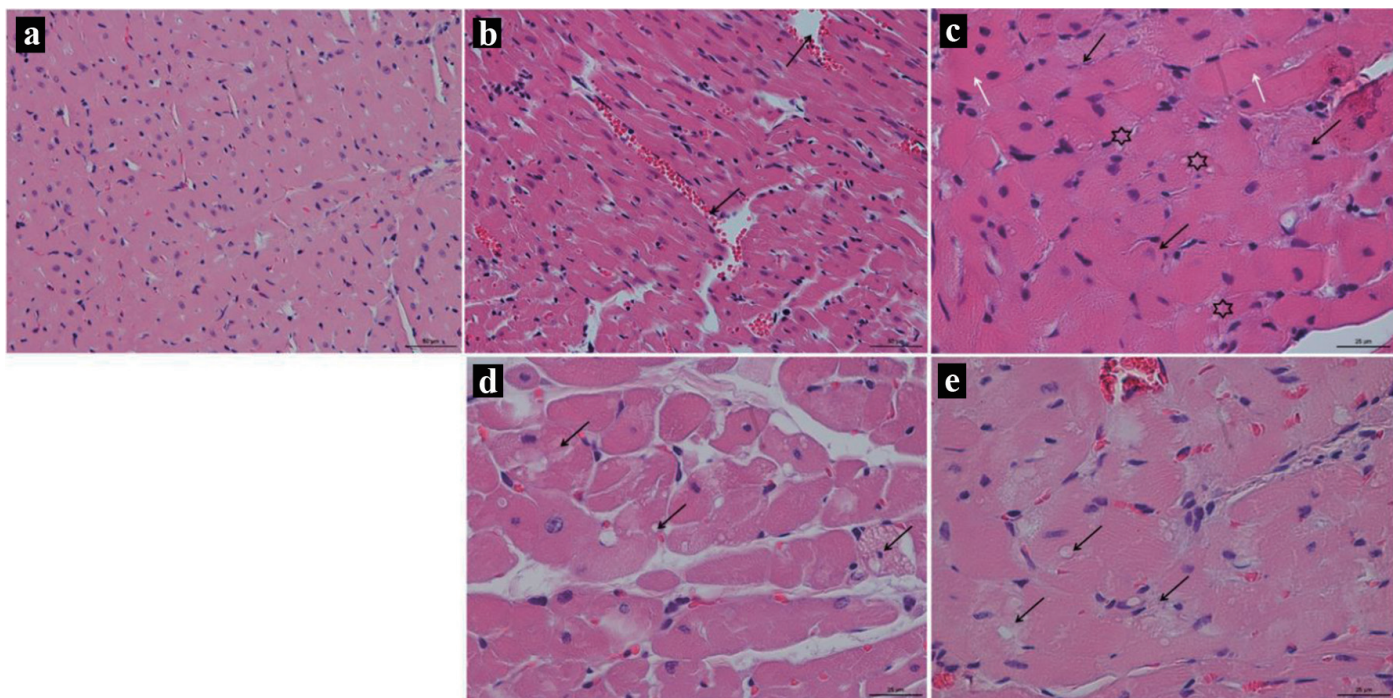


Figure 7. (a) Representative images of rat's left cardiac ventricle of the control group; × 50; stained by hematoxylin and eosin. (b, c) Representative images of rat's left cardiac ventricle of the DOX-15 group; stained by hematoxylin and eosin. (b) Dissociation of myocardial fibers is seen, forming cavities filled with blood (arrow); × 50. (c) Asterisks show vacuolization of the cytoplasm of cardiomyocytes, black arrows show nuclei of cardiocytes that undergo karyolysis, white arrows show hypertrophied fibers; × 25. (d) Representative images of rat's left cardiac ventricle of the DOX-10 group; × 25; stained by hematoxylin and eosin. Anisonucleosis, medium and large cell vacuolization of the cytoplasm (arrows). (e) Representative images of rat's left cardiac ventricle of the DOX-5 group; × 25; stained by hematoxylin and eosin. The arrows show vacuolization of the cytoplasm of cardiomyocytes, the absence of visible boundaries between individual cells.

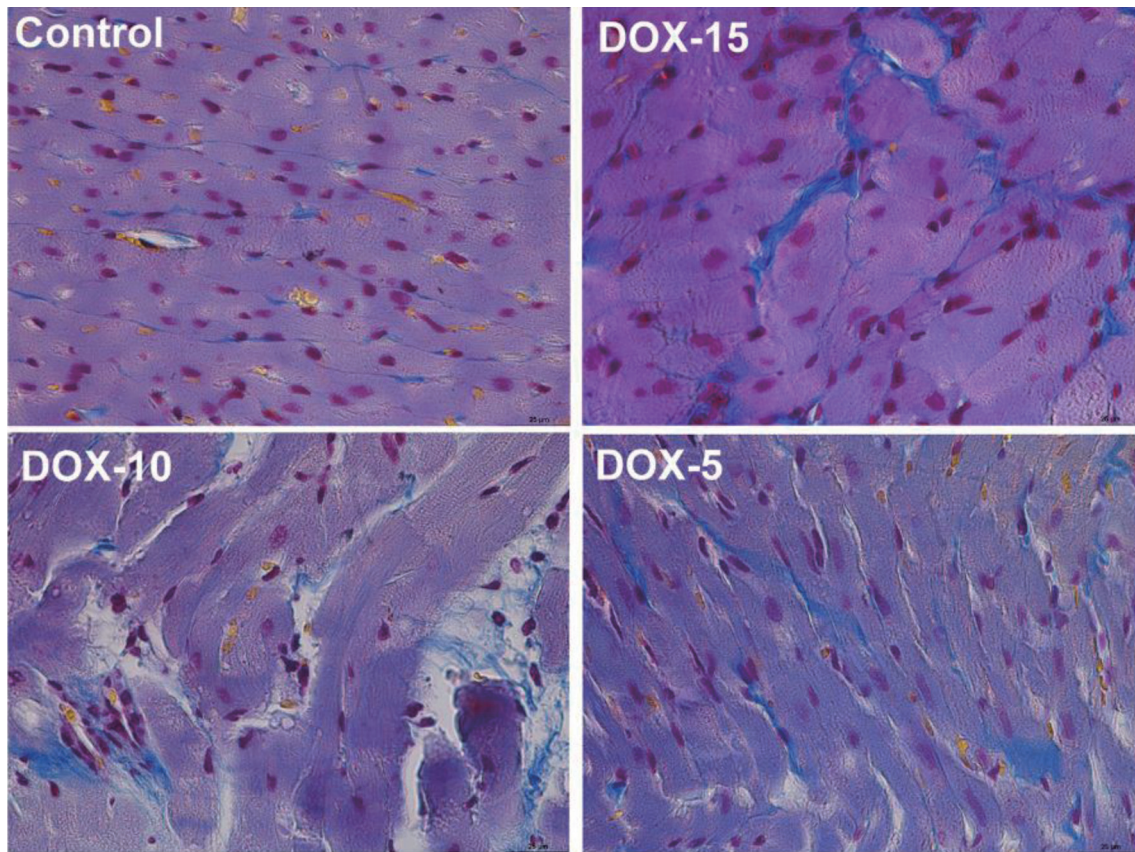


Figure 8. Representative images of rat's left cardiac ventricle of the control, DOX-15, DOX-10, and DOX-5 groups. Stained by Mallori, collagen is colored blue; × 25.

with 5 mg/kg of the drug compared to the control group. Due to a progressive doxorubicin-induced cardiomyopathy development and multiple vital organs failure (extensive necrosis

of hepatocytes, segmental glomerulosclerosis, necrosis of tubular epithelium) rats' intake 15 mg/kg of doxorubicin began to lose much weight 45 days after the end of injections, which was incompatible with life. This led to the ascites development for one animal, presumably due to a severe heart failure associated with cardiomyopathy, which is also a side effect of doxorubicin. Thus, a dose of 15 mg/kg causes a pronounced cardiotoxic effect.

Two months after the end of doxorubicin administration, an RT-qPCR analysis found no changes in mRNA level of myocardial TGF-β1 in all experimental groups compared to the control group (Fig. 11). Expression of COL1A1 and COL2A1 significantly increased in the DOX-15 group ($P < 0.01$); there were no changes in the DOX-10 group; in the group with the minimum cumulative dose of doxorubicin (5 mg/kg), the level of mRNA of both genes significantly decreased ($P < 0.001$). At the same time, a downregulation of COL3A1 expression was found in all treatment groups. Animals from the DOX-10 group were characterized by downregulation of FGF2 ($P < 0.05$). In turn, heart tissues of rats, consuming the maximum (15 mg/kg) and minimum (5 mg/kg) doses of doxorubicin, showed an upregulation of FGF4 ($P < 0.001$). The downregulation of metalloproteases MMP-1 and MMP-14 expressions was found in the DOX-15 group and DOX-5 group, respectively ($P < 0.001$). Interestingly, MMP-2 was not affected by drug treatments in any of the groups. In contrast to the effect of MMP-1,

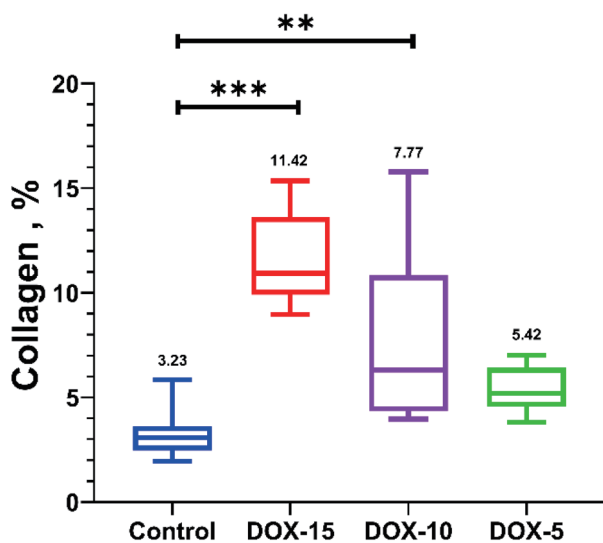


Figure 9. The amount of collagen in the left cardiac ventricle with chronic doxorubicin-induced cardiomyopathy of rats of the control, DOX-15, DOX-10, and DOX-5 groups, %. Kruskal-Wallis test.

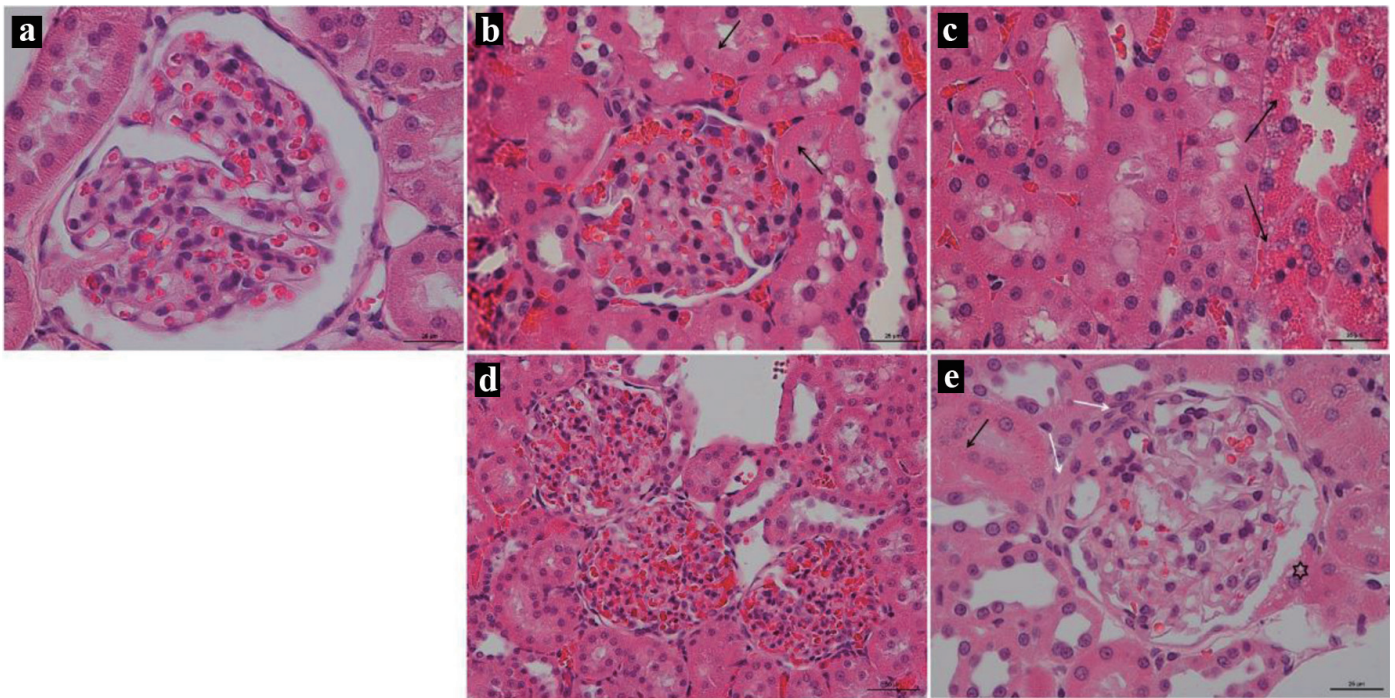


Figure 10. (a) Rat’s kidney of the Control group; × 25; stained by hematoxylin and eosin. (b, c) Rat’s kidney of the DOX-15 group; × 25; stained by hematoxylin and eosin. (b) The arrow shows the necrosis of the tubular epithelium, the sclerosed glomerulus shows in the center. (c) Massive tubular epithelial necrosis (arrow). (d) Rat’s kidney of the DOX-10 group; × 50; stained by hematoxylin and eosin. Global glomerulosclerosis of three renal glomeruli. (e) Rat’s kidney of the DOX-5 group; × 25; stained by hematoxylin and eosin. The black arrow shows necrosis of individual tubular epithelial cells. White arrows show thickening of the basement membrane of the glomerulus. Vacuolization of the cells of the parietal leaf of the capsule (asterisk).

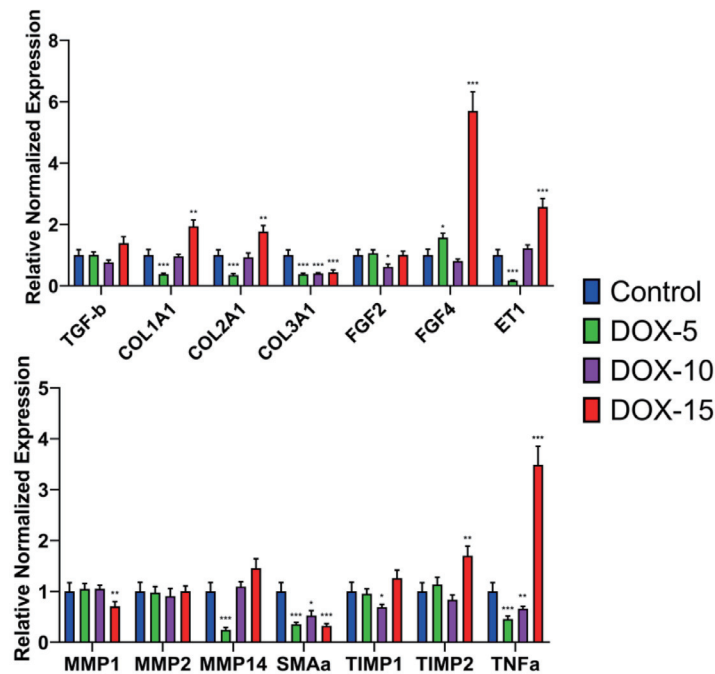


Figure 11. Gene expression levels of fibrotic molecular markers in the model of chronic doxorubicin-induced cardiomyopathy. *P < 0.05, **P < 0.01, ***P < 0.001 compared to control. COL1A1, COL2A1, COL3A1: collagen, type I, II, III; ET-1: endothelin-1; FGF: fibroblast growth factors; MMP: matrix metalloproteinases; TGF-β: transforming growth factor-β; TIMP: tissue inhibitor of metalloproteinase; TNF-α: tumor necrosis factor; α-SMA: alpha-smooth muscle actin.

mRNA level of TIMP-2 increased in the DOX-15 group ($P < 0.01$). At the same time, TIMP-1 expression decreased in the animals of the DOX-10 group ($P < 0.05$). Two months after the DOX-treatment, there was a significant increase in ET-1 in the group with the maximum cumulative dose ($P < 0.001$) and a significant decrease in animals receiving the minimum dose of the drug ($P < 0.001$). Expression of α -SMA was reduced dramatically in all experimental groups compared to the control group ($P < 0.001$). An increased mRNA level of TNF- α was specific only for the DOX-15 group animals ($P < 0.001$), while its expression is significantly down in the DOX-10 and DOX-5 groups ($P < 0.001$) (Fig. 11).

Discussion

This study is devoted to the development and verification of the acute and chronic model of doxorubicin-induced cardiomyopathy with fibrous myocardial damage and delayed development of diastolic dysfunction. The doxorubicin-induced cardiomyopathy pathogenesis is characterized by: 1) active accumulation of the drug in cardiomyocytes, which leads to excessive ROS generation, 2) development of inflammatory processes, 3) oxidative stress, which, in turn, disrupts the functioning of mitochondria, the sarcoplasmic reticulum, the balance of calcium and iron ions in the cell, 4) blocks the work of topoisomerase II β , and, ultimately, 5) causes the death of cardiomyocytes. The death of cardiomyocytes leads to their gradual replacement with fibrous tissue with diastolic dysfunction development.

To date, there has not been a final understanding of the mechanism for the anthracycline cardiomyopathy development, which makes it difficult to develop new methods of prevention and treatment despite the abundance of data on the various mechanisms involved in the doxorubicin-induced cardiotoxicity implementation. At the same time, researchers are actively trying to develop new models that provide a cardioprotective effect. For example, He et al demonstrated that repeated remote ischemic preconditioning eliminated the effects of doxorubicin-induced cardiotoxicity: it reduced the decline in cardiac function, weakened the formation of cardiac fibrosis, and reduced the processes development in cardiomyocytes [47]. Many modern works are aimed at stimulating sirtuins through various signaling pathways that have anti-inflammatory, antioxidant, anti-apoptotic effects on the myocardium [23, 48-50].

The study was performed on Wistar rats. The choice of this type of animals was motivated by a large number of published works devoted to doxorubicin cardiotoxic effects modeling in rats [40, 43, 51, 52]. In order to level the possibility of the influence of hormonal changes on the results obtained in the modeling of pathological processes, sexually mature males were used in this work.

The data obtained from the study indicate that a six-fold injection of 20 mg/kg doxorubicin provides manifestations of pronounced cardiotoxicity, manifested by a pronounced decrease in body weight of animals up to 20% in a short period of time, severe damage to both the cardiac muscle of the left

ventricle and the renal tissue, high mortality at the end of the experiment. Whereas the results of animals treated with 15 mg/kg of the drug showed a high survival rate. As a result, this dose was chosen as a “standard” for the chronic model of doxorubicin-induced cardiomyopathy development.

As the main criteria for verification of the chronic model of doxorubicin-induced cardiomyopathy with fibrous myocardial damage and delayed development of diastolic dysfunction, the authors used the following: the increase in the percentage of collagen; the degree of decrease of FS, which characterizes the pumping ability of the heart; clinical blood test, reflecting the toxic effect of the drug on hematopoiesis. To confirm fibrotic changes identified by histological analysis, an additional genetic analysis was carried out for the differential expression of fibrosis marker genes: TGF- β , COL1A1, COL2A1, COL3A1, FGF2, FGF4, α -SMA, TNF- α , ET-1, MMP-1, 2, 14, TIMP-1, 2.

To fulfill the task, a range of doxorubicin doses of 5 - 15 mg/kg was used, and the choice of doses was based on literature data [15]. The observation time after reaching the cumulative dose of the drug was 2 months, which is sufficient for the development of delayed effects of doxorubicin, myocardial fibrosis and diastolic dysfunction [53].

The results obtained showed that the administration of doxorubicin in doses of 10 and 15 mg/kg affected the physical condition and weight gain of the animals. A dose of 15 mg/kg of the drug caused weight loss against the background of a pronounced deterioration in the clinical condition of the animals, while the administration of 10 mg/kg of doxorubicin stopped the body weight gain, which could also be a manifestation of the toxic effect of doxorubicin. Moreover, with the administration of the drug in doses of 10 and 15 mg/kg, hematopoiesis inhibition was observed, which also indicates the toxic effect of doxorubicin. During the administration of all doses (5, 10 and 15 mg/kg), there was a significant decrease in FS, which reflects an impairment of the myocardium diastolic function, also affected by the resulting fibrous tissue. FS is the change in left ventricular size during each heartbeat expressed as a percentage and normally should not decrease by more than 10%. It is known from literature sources that one of the indicators of subclinical cardiotoxicity development determined via echocardiography in humans is a drop in both FS and ejection fraction [10, 54]. Therefore, as per the results of echocardiography, it can be concluded that doses of 10 and 5 mg/kg doxorubicin work best for creating chronic anthracycline cardiomyopathy since they contribute to a decrease in FS, but they are not critical for the life of the animal. The presence of fibrotic changes was confirmed by histological analysis. Thus, in animals receiving 10 and 15 mg/kg, a significant increase in the percentage of collagen in the heart muscle was revealed. The histological picture of the kidneys also demonstrated the presence of a nephrotoxic effect when using cumulative anthracycline doses of 10 and 15 mg/kg.

Two months after the end of chemotherapy administration, an analysis of fibrosis molecular markers showed that mRNA level of myocardial TGF- β did not change. At the same time, an increase in COL type I and II, FGF4 in animals that had received the highest dose of doxorubicin (15 mg/kg) remained. Whereas the amount of interstitial collagenase-1 (MMP-1)

was significantly reduced in animals of the DOX-15 group, which possibly correlates with TIMP2 activation. These results may indicate a temporary adjustment of the regulation of the TGF/FGF and MMP/TIMP systems during the formation of fibrous tissue against the background of the toxic effect of doxorubicin [55]. However, it was found that the excessive production of myocardial collagen type I and II (COL1A1 and COL2A1) persisted after 2 months in the DOX-15 group animals, while it did not change in the DOX-10 group animals, and it significantly decreased in the DOX-5 group animals. It can be assumed that 2 months after reaching the cumulative dose of doxorubicin, despite the absence of significant changes in TGF- β , the formation of fibrosis is not complete, and the preserved FGF4 expression may play a greater role in the development of chronic doxorubicin-induced cardiomyopathy. It is important to note a decline in type III myocardial collagen in all experimental groups. The main consequence of fibrosis is a fall in the ventricular compliance. Ventricular compliance decreases both due to an increase in the number of collagen fibers and as a result of the collagen properties variation. That is, a decrease in the content of “elastic” type III collagen and an increase in the content of “hard” type I collagen [60]. Thus, fibrosis progresses to the development of diastolic dysfunction.

It should be noted that the excess production of ET-1 persists after 2 months of observation in animals treated with 15 mg/kg of the drug, while a significant decrease in ET-1 was characteristic of animals of the DOX-5 group. A number of studies show that ET-1 can induce collagen synthesis in cardiac fibroblasts via the ETA receptor, and this effect was similar to that of TGF- β [56-58]. Our data support the role of ET-1 as a key player in cardiac fibrosis. In addition, an increase in TNF- α was revealed in the group of animals treated with 15 mg/kg of the drug, which indicates there are persisting inflammatory processes in the heart muscle. Whereas in animals of the DOX-10 and DOX-5 groups, a significant decrease in the inflammatory factor was observed 2 months after the end of its administration. This result confirms that a dose of 15 mg/kg doxorubicin is highly cardiotoxic. The fibrous factor α -SMA was reduced in all experimental groups, which may indicate that it may not be a significant marker of fibrous tissue formation in the development of chronic doxorubicin-induced cardiomyopathy [32, 59]. In general, the data obtained confirm the presence of fibrotic changes in the cardiac muscle.

The authors did not evaluate troponin and N-terminal pro B-type natriuretic peptide (NT-proBNP) levels for model verification since literature data indicate the ambiguity of the relationship between these criteria and the severity of myocardial damage under the action of doxorubicin [60-64]. A limited set of criteria was used to verify the acute model of doxorubicin-induced cardiomyopathy. These criteria are basic and sufficient to determine the optimal dose range for creating the chronic model of doxorubicin-induced cardiomyopathy.

Therefore, inflammatory processes and active synthesis of fibrous tissue that persisted after 2 months in animals treated with 15 mg/kg of doxorubicin correlate with a progressive deterioration of their clinical condition. This dose is highly cardiotoxic, which does not allow us to consider it suitable for creating chronic doxorubicin-induced cardiomyopathy. A dose of 10 mg/kg of the drug is associated with fibrotic changes and is

suitable for assessing chronic cardioprotective effects. A dose of 5 mg/kg of doxorubicin does not ensure the development of the processes of formation of fibrotic changes, and, consequently, cardiotoxicity. It is necessary to note the preserved expression of ET-1, FGF4 and TNF- α , which can affect the regulation of TGF- β , myocardial collagen types I, II, III and MMP/TIMP during the formation of chronic processes against the background of chemotherapy. This molecular genetic aspect remains to be studied in more detail, since understanding the interaction of fibrotic markers with each other can help in the development of methods for the prevention and treatment of anthracycline cardiotoxicity.

Conclusions

The optimal cumulative dose of doxorubicin leading to clinical manifestations confirmed by echocardiographic, histological, molecular changes associated with the development of chronic doxorubicin-induced cardiomyopathy with fibrotic lesions of the left ventricular of the cardiac muscle and ensuring long-term survival of animals is 10 mg/kg doxorubicin. The model with intraperitoneal administration of 10 mg/kg doxorubicin to Wistar rats can be used to study the mechanisms of development of anthracycline cardiotoxicity as close as possible to the changes that develop clinically in those people who have undergone chemotherapy.

Acknowledgments

None to declare.

Financial Disclosure

This work was financially supported by the Ministry of Science and Higher Education of the Russian Federation (agreement No. 075-15-2020-901).

Conflict of Interest

The authors confirm that they have no conflict of interest to declare.

Informed Consent

Not applicable.

Author Contributions

EP: conceptualization, investigation, data collection, analysis, writing - original draft preparation and editing; TS: material preparation, data collection, and writing - original draft preparation; EK: writing - original draft preparation; AO: material

preparation; MM: investigation; DA and RT: material preparation and data collection; YC: investigation; KL: editing; AG: editing; YT: conceptualization, editing, project administration, funding acquisition.

Data Availability

The authors declare that data supporting the findings of this study are available within the article.

References

1. Takemura G, Fujiwara H. Doxorubicin-induced cardiomyopathy from the cardiotoxic mechanisms to management. *Prog Cardiovasc Dis.* 2007;49(5):330-352.
2. Renu K, V GA, P BT, Arunachalam S. Molecular mechanism of doxorubicin-induced cardiomyopathy - An update. *Eur J Pharmacol.* 2018;818:241-253.
3. Wallace KB, Sardao VA, Oliveira PJ. Mitochondrial Determinants of Doxorubicin-Induced Cardiomyopathy. *Circ Res.* 2020;126(7):926-941.
4. Arcamone F, Cassinelli G, Fantini G, Grein A, Orezzi P, Pol C, Spalla C. Adriamycin, 14-hydroxydaunomycin, a new antitumor antibiotic from *S. peucetius* var. *caesius*. *Biotechnol Bioeng.* 1969;11(6):1101-1110.
5. Le Bot MA, Begue JM, Kernaleguen D, Robert J, Ratanasavanh D, Airiau J, Riche C, et al. Different cytotoxicity and metabolism of doxorubicin, daunorubicin, epirubicin, esorubicin and idarubicin in cultured human and rat hepatocytes. *Biochem Pharmacol.* 1988;37(20):3877-3887.
6. Arola OJ, Saraste A, Pulkki K, Kallajoki M, Parvinen M, Voipio-Pulkki LM. Acute doxorubicin cardiotoxicity involves cardiomyocyte apoptosis. *Cancer Res.* 2000;60(7):1789-1792.
7. Lu L, Wu W, Yan J, Li X, Yu H, Yu X. Adriamycin-induced autophagic cardiomyocyte death plays a pathogenic role in a rat model of heart failure. *Int J Cardiol.* 2009;134(1):82-90.
8. Zhang T, Zhang Y, Cui M, Jin L, Wang Y, Lv F, Liu Y, et al. CaMKII is a RIP3 substrate mediating ischemia- and oxidative stress-induced myocardial necroptosis. *Nat Med.* 2016;22(2):175-182.
9. Fang X, Wang H, Han D, Xie E, Yang X, Wei J, Gu S, et al. Ferroptosis as a target for protection against cardiomyopathy. *Proc Natl Acad Sci U S A.* 2019;116(7):2672-2680.
10. Plokhova EV, Doundoua DP. Cardiooncology. Basic principles of prevention and treatment of cardiotoxicity in cancer patients. *J Clin Pract.* 2019;10(1):30-40.
11. Corremans R, Adao R, De Keulenaer GW, Leite-Moreira AF, Bras-Silva C. Update on pathophysiology and preventive strategies of anthracycline-induced cardiotoxicity. *Clin Exp Pharmacol Physiol.* 2019;46(3):204-215.
12. Zhang S, Liu X, Bawa-Khalife T, Lu LS, Lyu YL, Liu LF, Yeh ET. Identification of the molecular basis of doxorubicin-induced cardiotoxicity. *Nat Med.* 2012;18(11):1639-1642.
13. Lyu YL, Kerrigan JE, Lin CP, Azarova AM, Tsai YC, Ban Y, Liu LF. Topoisomerase IIbeta mediated DNA double-strand breaks: implications in doxorubicin cardiotoxicity and prevention by dexrazoxane. *Cancer Res.* 2007;67(18):8839-8846.
14. Vejpongsa P, Yeh ET. Topoisomerase 2beta: a promising molecular target for primary prevention of anthracycline-induced cardiotoxicity. *Clin Pharmacol Ther.* 2014;95(1):45-52.
15. Podyacheva EY, Kushnareva EA, Karpov AA, Toropova YG. Analysis of Models of Doxorubicin-Induced Cardiomyopathy in Rats and Mice. A Modern View From the Perspective of the Pathophysiologist and the Clinician. *Front Pharmacol.* 2021;12:670479.
16. Salazar-Mendiguchia J, Gonzalez-Costello J, Roca J, Ariza-Sole A, Manito N, Cequier A. Anthracycline-mediated cardiomyopathy: basic molecular knowledge for the cardiologist. *Arch Cardiol Mex.* 2014;84(3):218-223.
17. Octavia Y, Tocchetti CG, Gabrielson KL, Janssens S, Crijns HJ, Moens AL. Doxorubicin-induced cardiomyopathy: from molecular mechanisms to therapeutic strategies. *J Mol Cell Cardiol.* 2012;52(6):1213-1225.
18. Kim SJ, Kim HS, Seo YR. Understanding of ROS-inducing strategy in anticancer therapy. *Oxid Med Cell Longev.* 2019;2019:5381692.
19. Russo M, Della Sala A, Tocchetti CG, Porporato PE, Ghiogo A. Metabolic aspects of anthracycline cardiotoxicity. *Curr Treat Options Oncol.* 2021;22(2):18.
20. Nebigil CG, Desaubry L. Updates in anthracycline-mediated cardiotoxicity. *Front Pharmacol.* 2018;9:1262.
21. Menna P, Paz OG, Chello M, Covino E, Salvatorelli E, Minotti G. Anthracycline cardiotoxicity. *Expert Opin Drug Saf.* 2012;11(Suppl 1):S21-36.
22. Podyacheva E, Toropova Y. Nicotinamide riboside for the prevention and treatment of doxorubicin cardiomyopathy. *Opportunities and Prospects. Nutrients.* 2021;13(10):3435.
23. Wang AJ, Zhang J, Xiao M, Wang S, Wang BJ, Guo Y, Tang Y, et al. Molecular mechanisms of doxorubicin-induced cardiotoxicity: novel roles of sirtuin 1-mediated signaling pathways. *Cell Mol Life Sci.* 2021;78(7):3105-3125.
24. Mawad W, Mertens L, Pagano JJ, Riesenkampff E, Reichert MJE, Mital S, Kantor PF, et al. Effect of anthracycline therapy on myocardial function and markers of fibrotic remodelling in childhood cancer survivors. *Eur Heart J Cardiovasc Imaging.* 2021;22(4):435-442.
25. Vejpongsa P, Yeh ET. Prevention of anthracycline-induced cardiotoxicity: challenges and opportunities. *J Am Coll Cardiol.* 2014;64(9):938-945.
26. Mascia G, Arbelo E, Porto I, Brugada R, Brugada J. The arrhythmogenic right ventricular cardiomyopathy in comparison to the athletic heart. *J Cardiovasc Electrophysiol.* 2020;31(7):1836-1843.
27. Chatterjee K, Zhang J, Honbo N, Karliner JS. Doxorubicin cardiomyopathy. *Cardiology.* 2010;115(2):155-162.
28. Fraccarollo D, Galuppo P, Bauersachs J, Ertl G. Collagen accumulation after myocardial infarction: effects of ETA receptor blockade and implications for early remodeling.

- Cardiovasc Res. 2002;54(3):559-567.
29. Pan X, Chen Z, Huang R, Yao Y, Ma G. Transforming growth factor beta1 induces the expression of collagen type I by DNA methylation in cardiac fibroblasts. *PLoS One*. 2013;8(4):e60335.
 30. Rolski F, Blyszczuk P. Complexity of TNF- α signaling in heart disease. *J Clin Med*. 2020;9(10):1-25.
 31. Murphy SP, Kakkar R, McCarthy CP, Januzzi JL, Jr. Inflammation in Heart Failure: JACC State-of-the-Art Review. *J Am Coll Cardiol*. 2020;75(11):1324-1340.
 32. Zhao W, Wang X, Sun KH, Zhou L. α -smooth muscle actin is not a marker of fibrogenic cell activity in skeletal muscle fibrosis. *PLoS One*. 2018;13(1):e0191031.
 33. Herrera J, Henke CA, Bitterman PB. Extracellular matrix as a driver of progressive fibrosis. *J Clin Invest*. 2018;128(1):45-53.
 34. Ma ZG, Yuan YP, Wu HM, Zhang X, Tang QZ. Cardiac fibrosis: new insights into the pathogenesis. *Int J Biol Sci*. 2018;14(12):1645-1657.
 35. Bardi E, Bobok I, A VO, Kappelmayer J, Kiss C. Anthracycline antibiotics induce acute renal tubular toxicity in children with cancer. *Pathol Oncol Res*. 2007;13(3):249-253.
 36. Fujimura T, Yamagishi S, Ueda S, Fukami K, Shibata R, Matsumoto Y, Kaida Y, et al. Administration of pigment epithelium-derived factor (PEDF) reduces proteinuria by suppressing decreased nephrin and increased VEGF expression in the glomeruli of adriamycin-injected rats. *Nephrol Dial Transplant*. 2009;24(5):1397-1406.
 37. Ramadan R, Faour D, Awad H, Khateeb E, Cohen R, Yahia A, Torgovicky R, et al. Early treatment with everolimus exerts nephroprotective effect in rats with adriamycin-induced nephrotic syndrome. *Nephrol Dial Transplant*. 2012;27(6):2231-2241.
 38. Wu Q, Li W, Zhao J, Sun W, Yang Q, Chen C, Xia P, et al. Apigenin ameliorates doxorubicin-induced renal injury via inhibition of oxidative stress and inflammation. *Biomed Pharmacother*. 2021;137:111308.
 39. Lee VW, Harris DC. Adriamycin nephropathy: a model of focal segmental glomerulosclerosis. *Nephrology (Carlton)*. 2011;16(1):30-38.
 40. Nakahara T, Tanimoto T, Petrov AD, Ishikawa K, Strauss HW, Narula J. Rat model of cardiotoxic drug-induced cardiomyopathy. *Methods Mol Biol*. 2018;1816:221-232.
 41. Hamm C, Fifield BA, Kay A, Kulkarni S, Gupta R, Mathews J, Ferraiuolo RM, et al. A prospective phase II clinical trial identifying the optimal regimen for carboplatin plus standard backbone of anthracycline and taxane-based chemotherapy in triple negative breast cancer. *Med Oncol*. 2022;39(4):49.
 42. Zbinden G, Bachmann E, Holderegger C. Model systems for cardiotoxic effects of anthracyclines. *Antibiot Chemother (1971)*. 1978;23:255-270.
 43. Medeiros-Lima DJM, Carvalho JJ, Tibirica E, Borges JP, Matsuura C. Time course of cardiomyopathy induced by doxorubicin in rats. *Pharmacol Rep*. 2019;71(4):583-590.
 44. Aygun H, Gul SS. Cardioprotective effect of melatonin and agomelatine on doxorubicin-induced cardiotoxicity in a rat model: an electrocardiographic, scintigraphic and biochemical study. *Bratisl Lek Listy*. 2019;120(4):249-255.
 45. Aykan DA, Yaman S, Eser N, Ozcan Metin T, Seyithanoglu M, Aykan AC, Kurt AH, et al. Bisoprolol and linagliptin ameliorated electrical and mechanical isometric myocardial contractions in doxorubicin-induced cardiomyopathy in rats. *Pharmacol Rep*. 2020;72(4):867-876.
 46. Ivanova M, Dovinova I, Okruhlicova L, Tribulova N, Simoncikova P, Bartekova M, Vlkovicova J, et al. Chronic cardiotoxicity of doxorubicin involves activation of myocardial and circulating matrix metalloproteinases in rats. *Acta Pharmacol Sin*. 2012;33(4):459-469.
 47. He Q, Wang F, Ryan TD, Chalasani M, Redington AN. Repeated Remote Ischemic Conditioning Reduces Doxorubicin-Induced Cardiotoxicity. *JACC CardioOncol*. 2020;2(1):41-52.
 48. Hu C, Zhang X, Song P, Yuan YP, Kong CY, Wu HM, Xu SC, et al. Meteorin-like protein attenuates doxorubicin-induced cardiotoxicity via activating cAMP/PKA/SIRT1 pathway. *Redox Biol*. 2020;37:101747.
 49. Li D, Yang Y, Wang S, He X, Liu M, Bai B, Tian C, et al. Role of acetylation in doxorubicin-induced cardiotoxicity. *Redox Biol*. 2021;46:102089.
 50. Han D, Wang Y, Wang Y, Dai X, Zhou T, Chen J, Tao B, et al. The Tumor-Suppressive Human Circular RNA CircITCH Sponges miR-330-5p to Ameliorate Doxorubicin-Induced Cardiotoxicity Through Upregulating SIRT6, Survivin, and SERCA2a. *Circ Res*. 2020;127(4):e108-e125.
 51. Loncar-Turukalo T, Vasic M, Tasic T, Mijatovic G, Glumac S, Bajic D, Japunzic-Zigon N. Heart rate dynamics in doxorubicin-induced cardiomyopathy. *Physiol Meas*. 2015;36(4):727-739.
 52. Merlet N, Piriou N, Rozec B, Grabherr A, Lauzier B, Trochu JN, Gauthier C. Increased beta2-adrenoceptors in doxorubicin-induced cardiomyopathy in rat. *PLoS One*. 2013;8(5):e64711.
 53. Mehdipoor M, Damirchi A, Razavi Tousi SMT, Babaei P. Concurrent vitamin D supplementation and exercise training improve cardiac fibrosis via TGF-beta/Smad signaling in myocardial infarction model of rats. *J Physiol Biochem*. 2021;77(1):75-84.
 54. Markham MJ, Wachter K, Agarwal N, Bertagnolli MM, Chang SM, Dale W, Diefenbach CSM, et al. Clinical Cancer Advances 2020: Annual Report on Progress Against Cancer From the American Society of Clinical Oncology. *J Clin Oncol*. 2020;38(10):1081.
 55. Aharinejad S, Krenn K, Paulus P, Schafer R, Zuckermann A, Grimm M, Abraham D. Differential role of TGF-beta1/bFGF and ET-1 in graft fibrosis in heart failure patients. *Am J Transplant*. 2005;5(9):2185-2192.
 56. Hafizi S, Wharton J, Chester AH, Yacoub MH. Profibrotic effects of endothelin-1 via the ETA receptor in cultured human cardiac fibroblasts. *Cell Physiol Biochem*. 2004;14(4-6):285-292.
 57. Sernerer GG, Cecioni I, Vanni S, Paniccia R, Bandinelli B, Vetere A, Janming X, et al. Selective upregulation of cardiac endothelin system in patients with ischemic but not idiopathic dilated cardiomyopathy: endothelin-1 system

- in the human failing heart. *Circ Res.* 2000;86(4):377-385.
58. Remuzzi G, Perico N, Benigni A. New therapeutics that antagonize endothelin: promises and frustrations. *Nat Rev Drug Discov.* 2002;1(12):986-1001.
 59. Sun KH, Chang Y, Reed NI, Sheppard D. alpha-Smooth muscle actin is an inconsistent marker of fibroblasts responsible for force-dependent TGFbeta activation or collagen production across multiple models of organ fibrosis. *Am J Physiol Lung Cell Mol Physiol.* 2016;310(9):L824-836.
 60. Chan BYH, Roczkowsky A, Moser N, Poirier M, Hughes BG, Ilarraza R, Schulz R. Doxorubicin induces de novo expression of N-terminal-truncated matrix metalloproteinase-2 in cardiac myocytes. *Can J Physiol Pharmacol.* 2018;96(12):1238-1245.
 61. Lu X, Zhao Y, Chen C, Han C, Xue L, Xing D, Huang O, et al. BNP as a marker for early prediction of anthracycline-induced cardiotoxicity in patients with breast cancer. *Oncol Lett.* 2019;18(5):4992-5001.
 62. Zidan A, Sherief LM, El-sheikh A, Saleh SH, Shahbah DA, Kamal NM, Sherbiny HS, et al. NT-proBNP as early marker of subclinical late cardiotoxicity after doxorubicin therapy and mediastinal irradiation in childhood cancer survivors. *Dis Markers.* 2015;2015:513219.
 63. Advani P, Hoyne J, Moreno-Aspita A, Dubin M, Brock S, Harlow C, Chumsri S, et al. High-Sensitivity Troponin T and NT-proBNP Kinetics in Breast Cancer Chemotherapy. *Chemotherapy.* 2017;62(6):334-338.
 64. Argun M, Uzum K, Sonmez MF, Ozyurt A, Derya K, Cilenk KT, Unalmis S, et al. Cardioprotective effect of metformin against doxorubicin cardiotoxicity in rats. *Anatol J Cardiol.* 2016;16(4):234-241.